Title

Equatorial coordination of uranyl: Correlating ligand charge donation with the Oyl-U-Oyl asymmetric stretch frequency

Authors

Gibson, John K
de Jong, Wibe A
van Stipdonk, Michael J
et al.

Publication Date

2018-02-01

DOI

10.1016/j.jorganchem.2017.10.010

Peer reviewed

Equatorial Coordination of Uranyl: Correlating Ligand Charge Donation with the O_{yl}-U-O_{yl} Asymmetric Stretch Frequency

John K. Gibson,[1,*] Wibe A. de Jong,[2,*] Michael J. van Stipdonk,[3]
Jonathan Martens,[4] Giel Berden,[4] Jos Oomens[4,5]

[1] *Chemical Sciences Division, Lawrence Berkeley National Laboratory, Berkeley, California 94720, USA*
[2] *Computational Research Division, Lawrence Berkeley National Laboratory, Berkeley, California 94720, USA*
[3]*Department of Chemistry and Biochemistry, Duquesne University, Pittsburgh, Pennsylvania 15282, USA*
[4]*Radboud University, Institute for Molecules and Materials, FELIX Laboratory, Toernooiveld 7c, 6525ED Nijmegen, The Netherlands*
[5]*Van't Hoff Institute for Molecular Sciences, University of Amsterdam, Science Park 904, 1098XH Amsterdam, The Netherlands*

Corresponding authors email: jkgibson@lbl.gov; wadejong@lbl.gov

Keywords: Uranyl; Coordination complexes: Gas-phase; IRMPD; Proton affinity

Abstract

In uranyl coordination complexes, $UO_2(L)_n^{2+}$, uranium in the *formally* dipositive $[O=U=O]^{2+}$ moiety is coordinated by *n* neutral organic electron donor ligands, L. The extent of ligand electron donation, which results in partial reduction of uranyl and weakening of the U=O bonds, is revealed by the magnitude of the red-shift of the uranyl asymmetric stretch frequency, ν_3. This phenomenon appears in gas-phase complexes in which uranyl is coordinated by electron donor ligands: the ν_3 red-shift increases as the number of ligands and their proton affinity (PA) increases. Because PA is a measure of the enthalpy change associated with a proton-ligand interaction, which is much stronger and of a different nature than metal ion-ligand bonding, it is not necessarily expected that ligand PAs should reliably predict uranyl-ligand bonding and the resulting ν_3 red-shift. Here, ν_3 was measured for uranyl coordinated by ligands with a relatively broad range of PAs, revealing a surprisingly good correlation between PA and ν_3 frequency From computed ν_3 frequencies for bare UO_2 cations and neutrals, it is inferred that the effective charge of uranyl in $UO_2(L)_n^{2+}$ complexes can be reduced to near zero upon ligation by sufficiently strong charge-donor ligands. The basis for the correlation between ν_3 and ligand PAs, as well as limitations and deviations from it, are considered. It is demonstrated that the correlation evidently extends to a ligand that exhibits polydentate metal ion coordination.

1. Introduction

It is known that the uranium-oxygen bonds in the uranyl dication, UO_2^{2+}, are weakened by electron donation to the uranium metal center by coordinating nucleophiles.[1-4] The origins of this phenomenon are generally attributed to partial reduction of U(VI) with concomitant occupation of 5f orbitals, although other explanations have been proposed.[5] However, understanding the underlying basis for the effects of coordinating ligands on uranium-oxygen bonding in uranyl is complicated by the many competing and uncertain interactions in condensed phases.[6] Accordingly, Groenewold, Van Stipdonk and coworkers[7] employed infrared multiphoton dissociation (IRMPD) spectroscopy of isolated gas-phase uranyl-ligand (L) complexes, $UO_2(L)_n^{2+}$, to evaluate the effects of ligation alone on the U-O bonding, unaffected by complexities introduced in solutions and solids. It was demonstrated in that work that the uranyl asymmetric stretch frequency, ν_3, decreases as the number of electron donating ligands, *n*, increases, and also that ν_3 decreases as the ligand nucleophilicity increases from L = acetonitrile (acn) to L = acetone (aco). These results demonstrated an intrinsic red-shift in ν_3 as a result of electron donation in elementary systems, and furthermore that this effect could be accurately modeled by ab initio quantum chemistry computations.

In view of the demonstration by Groenewold et al. of the effects of ligand electron donation on uranium-oxygen bonding in gas-phase uranyl complexes, and the resulting ν_3 red-shift, it is desirable to extend this line of inquiry to better understand and quantify factors that determine the diminution of O=U=O bonding as revealed by ν_3. A challenge is to identify a ligand parameter that reliably correlates with charge donation to metal ions in general, and uranyl in particular. Gas-phase reaction (1) has been studied for numerous neutral organic molecules, denoted as ligand L in the present context.[8]

$$L + H^+ \rightarrow LH^+ \quad (1)$$

The proton affinity (PA) of L is defined as a positive value and is the negative of the enthalpy of reaction (1), $PA[L] = -\Delta_{Reaction(1)}H^o_{298}$; ligand gas basicity (GB) is the corresponding free energy, $GB[L] = -\Delta_{Reaction(1)}G^o_{298}$. The quantity PA[L] is thus a direct measure of the bond dissociation energy for LH^+: $D[L\text{-}H^+] = PA[L]$. Although PA[L] is a measure of affinity of L for a specific cation, H^+, it is not necessarily generally indicative of the affinity of L for other cations, notably metal ions. As the smallest monopositive metal ion, Li^+ might be expected to exhibit similar affinities for ligands as does H^+. However, the $L\text{-}H^+$ bonding interaction is highly covalent

whereas that between L and Li^+, as well as other metal cations, is primarily electrostatic.[9,10] As a result, PAs are generally much larger than metal cation affinities (MCAs), including lithium cation affinities, LCA[L] = $-\Delta_{Reaction(2)}H^o_{298}$.

$$L + Li^+ \rightarrow LLi^+ \qquad (2)$$

For acetonitrile, PA[acn] = 779 kJ/mol and LCA[acn] = 177 kJ/mol.[10] Very large disparities from PA are found for other LCA[L],[10] as well as other MCA[L].[11] In addition to the very large disparity in the magnitudes of PAs and MCAs, the correlation between the two quantities is rather poor.[10]

Groenewold et al.[7] did identify a correlation between the red-shift of the uranyl ν_3 frequency and the PAs of two ligands: PA[acn] = 779 kJ/mol and PA[aco] = 812 kJ/mol; ν_3 decreased as PA[L] increased. Given that the previous study was limited to two ligands, acn and aco, with rather similar PAs, in the present work the uranyl ν_3 frequency was determined for several $UO_2(L)_3^{2+}$ complexes comprising ligands with PAs spanning a much broader range, from PA[acn] = 779 kJ/mol to PA[tmtu] = 948 kJ/mol (tmtu = tetramethylthiourea). Although there is a clear correlation between ν_3 and PA[L], the results reveal that the relationship is flawed at a detailed level. The focus of this study is on ligands that bind to cations, specifically protons and metal ions, in a monodentate manner. However, it is also demonstrated that the relationship between PA and ν_3 appears to qualitatively apply in a case where uranyl binds to a ligand in a polydentate manner that is not feasible for a proton.

2. Experimental Methods

Using a stock solution of 10 mM uranyl perchlorate in water, a solution of 1 mM UO_2^{2+} methanol with 10% water was prepared for ESI in the IRMPD experiments. The ligand was added to the ESI solutions at relatively high concentrations (e.g. 10% by volume) for the comparatively weakly binding nitrile ligands, and at lower concentrations (e.g. 1%) for the other more strongly binding ligands. Previously established methods for generation of ions and the subsequent collection of IRMPD spectra at the Free Electron Laser for Infrared eXperiments (FELIX) Laboratory were used here.[7,12,13] Briefly, ESI was performed using a Micromass Z-Spray source; dry nitrogen at ~80 °C was used to assist desolvation. Ions were injected into a home-built Fourier transform ion cyclotron resonance (FT-ICR) mass spectrometer described elsewhere.[14] Ions were accumulated for the duration of the previous FT-ICR cycle (6 s) in an

external hexapole and injected into the ICR cell via a quadrupole deflector and an octapole RF ion guide. For each ligand, instrument operating parameters, such as desolvation temperature, cone voltage, and ion accumulation and transfer optics voltages, were optimized to maximize formation and transfer of the $UO_2(L)_4^{2+}$ ion, which was easier to form than the $UO_2(L)_3^{2+}$ ion. The extra ligand was then removed by irradiating the $UO_2(L)_4^{2+}$ ion for 0.01-1.3 s (depending on the ligand) with a 35 W continuous wave CO_2 laser, giving the $UO_2(L)_3^{2+}$ ion which was subsequently mass isolated.

Infrared spectra were recorded by measuring the photodissociation yield as a function of photon wavelength. Precursor ions were irradiated using 25 FELIX macropulses (55 mJ per macropulse, 5 μs pulse duration, fwhm bandwidth ~0.5% of central λ). In the IRMPD process, a photon is absorbed when the laser frequency matches a vibrational mode of the gas-phase ion and its energy is subsequently distributed over all vibrational modes by intramolecular vibrational redistribution (IVR).[15] The IVR process allows the energy of each photon to be dissipated before the ion absorbs another, which leads to promotion of ion internal energy toward the dissociation threshold via multiple photon absorption. Infrared spectra obtained using IRMPD are comparable to those collected using linear absorption techniques.[14,16-18] For these experiments, the FEL wavelength was tuned in 5 cm^{-1} increments over various ranges for different complexes, from as narrow as 9.3 μm (1080 cm^{-1}) to 10.4 μm (960 cm^{-1}), to as wide as 5.7 μm (1750 cm^{-1}) to 11.4 μm (880 cm^{-1}). The range was always sufficient to clearly identify the uranyl asymmetric stretch frequency of interest. The intensities of product and undissociated precursor ions were obtained from an averaged mass spectrum measured using the excite/detect sequence of the FT-ICR-MS after each IRMPD step. The IRMPD yield was normalized to the total ion current and linearly normalized for variations in the laser intensity.

3. Computational Methods

All the calculations in the manuscript were performed with version 6.6 of the open-source NWChem software suite.[19] Density functional theory calculations were carried out with the LDA[20,21] and B3LYP[22,23] density functional, using the Stuttgart small-core effective core-potentials and their associated basis sets for the actinide atoms[24] and all-electron DFT optimized valence triple-ζ polarized (TZVP) basis sets[25] for the first- and second row atoms in the complexes considered in this work. The geometries of the complexes were optimized without

symmetry constraints, followed by frequency calculations to ensure the calculated structure had no imaginary frequencies and was in a minimum energy configuration. Enthalpy corrections as computed by NWChem at 298K, using standard ideal gas phase partition functions,[26] were used to compute the enthalpies necessary for the determination of proton affinities. The calculated frequencies obtained with the B3LYP functional, which are well known to be overestimated,[27] and were empirically scaled by 0.975. All calculated energetics presented in this paper include the zero-point energy correction using the calculated and unscaled frequencies for LDA and B3LYP. The infrared spectrum was generated by applying a Gaussian broadening (10 cm^{-1} full width at half maximum) to each calculated peak with the peak height determined by its calculated intensity.

4. Results and Discussion

Complexes with composition $UO_2(L)_3^{2+}$ were studied for the following ligands L: acetonitrile (acn), propionitrile (pn), dimethylformamide (dmf), dimethylsulfoxide (dmso), tetramethylurea (tmu), and tetramethylthiourea (tmtu); previous results for the $UO_2(aco)_3^{2+}$ (aco = acetone) complex[7] are included in the evaluation. Computations were performed in this work for all of the complexes. The three-ligand uranyl complexes were studied because they could be produced for all ligands and, with one exception noted below, exhibit exclusively monodentate coordination to the uranium metal center of uranyl. These conditions allow for direct comparison of variations in uranyl-ligand binding. The ligand PAs are given in Table 1.

Table 1. Experimental and computed (LDA and B3LYP functional) ν_3 frequencies (cm^{-1}) for $UO_2(L)_3^{2+}$ complexes, and ligand L proton affinities (kJ/mol).

		ν_3 Computed[c]		Ligand PA	
Ligand L[a]	**ν_3 Experiment**[b]	**LDA**	**B3LYP**	**Computed B3LYP**	**Experiment**[d]
acn	1017	1031	1029	786.5	787.4
pn	1016	1026	1024	795.7	794.1
aco	1000[b]	1006	1007	814.6	812
dmf	979	975	980	887.7	887.5
dmso	973	958	974	899.2	884.4
tmu	956	945	957	927.5	930.6
tmtu	954	940[e]	954[e]	945.3	947.6

[a]acn = acetonitrile; pn = propionitrile; aco = acetone; dmf = dimethylformamide; dmso = dimethylsulfoxide; tmu = tetramethylurea; tmtu = tetramethylthiourea

[b]The experimental ν_3 for $UO_2(aco)_3^{2+}$ is taken from ref.[7]. The uncertainties in the experimental ν_3 values are estimated as ±2 cm^{-1}.

[c]The computed ν_3 at the B3LYP level of theory have been empirically scaled by 0.975.

[d]PAs at 298 K from ref.[28] except for acn from ref.[29] The uncertainties in the relative PAs are conservatively assigned as ±8 kJ/mol

[e]Frequencies listed are for the complex with one ligand bidentate bonded through both S and N, while the remaining two ligands are bonded monodentate through S only. The tmtu complex with all ligands bonded monodentate has a computed ν_3 of 962 cm^{-1}.

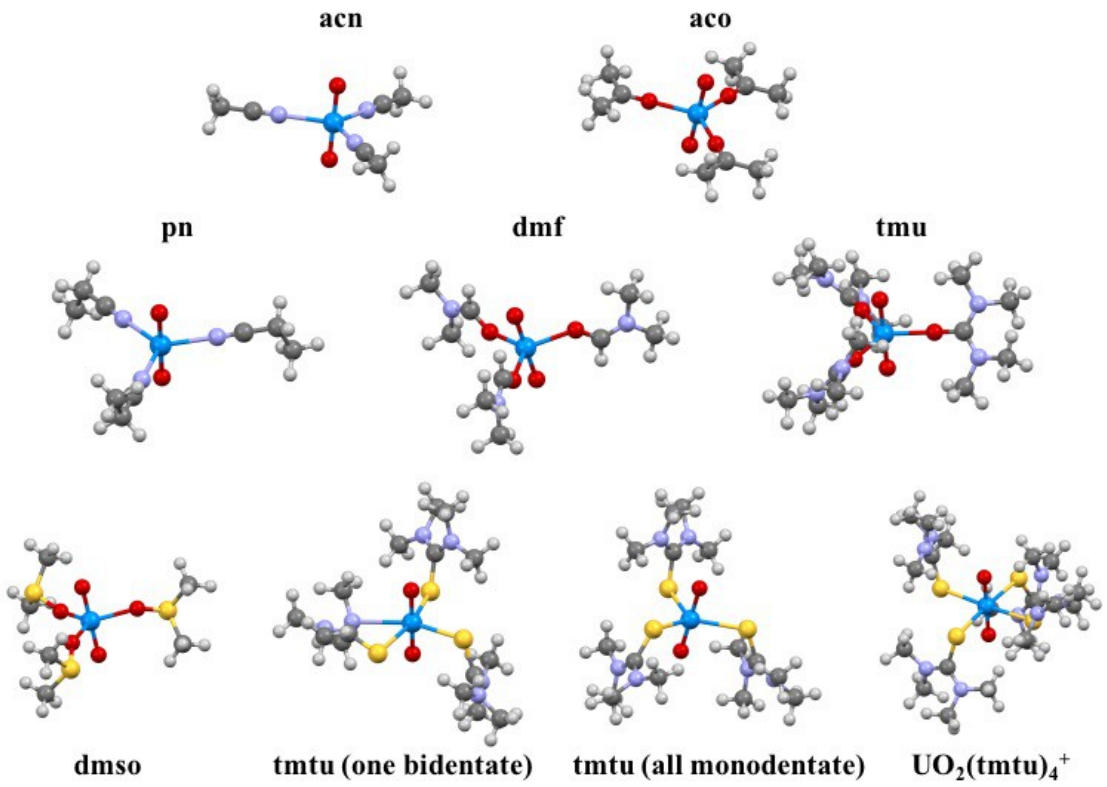

Figure 1. Computed structures of $UO_2(L)_3^{2+}$ complexes for L = acetonitrile (acn), acetone (aco), propionitrile (pn), dimethylsulfoxide (dmso), dimethylformamide (dmf), tetramethylurea (tmu), and tetramethylthiourea (tmtu). The tmtu complexes is shown in the two energetically competitive configurations. The structure of $UO_2(tmtu)_4^{2+}$ is included to show the change in coordination to all monodentate tmtu ligands. The U=O_{yl} and U-L_{eq} bond distances are in Table 2.

4.1 Computed Structures of $UO_2(L)_3^{2+}$ Complexes

The computed structures of $UO_2(L)_3^{2+}$ complexes are shown in Figure 1. The U=O_{yl} and U-O_{eq}, U-N_{eq} and U-S_{eq} distances are given in Table 2, where O_{yl} are the O=U=O uranyl oxygen atoms and the other atoms are those that coordinate uranyl in the equatorial plane. The structures of $UO_2(acn)_3^{2+}$ and $UO_2(aco)_3^{2+}$, reported previously,[7] are similar to that of $UO_2(pn)_3^{2+}$, with all three ligands bound to the uranium metal center through a nitrile N atom or acetone O atom, with simple monodentate coordination. The other complexes similarly exhibit monodentate coordination, with the exception of $UO_2(tmtu)_3^{2+}$ where a monodentate and bidentate structure are found within 8 kJ/mol of each other at the B3LYP level of theory, with the bidentate being the lower of the two. At the LDA level of theory the monodentate complex is found to be 16 kJ/mol lower in energy instead. The monodentate tmtu complex coordinates through the

thioketone S atom, while the bidentate complex is coordinated to uranium by both a thioketone S atom and a thioamide N atom. Because protons generally bind to one nucleophilic site in a molecule,[8] this unexpected bidentate coordination of tmtu to uranium is exemplary as to why PAs should not necessarily correlate well with MCAs when a second coordinating electron donor such as N is present in the ligand. The computed structure of $UO_2(tmtu)_4^{2+}$, shown in Figure 1, indicates that all four tmtu ligands are monodentate with the S atoms coordinated to uranium. The change from a competitive monodentate and bidentate bonding of the ligand in $UO_2(tmtu)_3^{2+}$ to all monodentate in $UO_2(tmtu)_4^{2+}$ is attributed to increasing steric congestion in the uranyl equatorial plane as the number of ligands increases from three to four.

Table 2. Selected computed bond distances (Å) in $UO_2(L)_3^{2+}$ complexes obtained with the B3LYP DFT functional.[a]

L	$U=O_{yl}$	$U-O_{eq}$	$U-S_{eq}$	$U-N_{eq}$
acn	1.739	-	-	2.446
pn	1.741	-	-	2.438
aco	1.749	2.308	-	-
dmso	1.761/1.765	2.276/2.274/2.277	-	-
dmf	1.762/1.758	2.297/2.297/2.296	-	-
tmu	1.768	2.258	-	-
tmtu (one bidentate) tmtu (all monodentate)	1.770/1.768 1.768/1.762	- -	2.788/2.863/2.746 2.762/2.760/2.742	2.714 -

[a]Structures are shown in Figure 1. The distances are the same for the two $U=O_{yl}$ distances where only one is given, and are the same for the three $U-O_{eq}$ or $U-N_{eq}$ distances where only one is given. As a reference, the $U=O_{yl}$ bond lengths calculated for the free UO_2^{2+}, UO_2^{+}, and UO_2 at the B3LYP level of theory are 1.701, 1.760 and 1.784 respectively.

4.2 Experimental and Computed IR Spectra of $UO_2(L)_3^{2+}$ Complexes

Experimental IRMPD spectra are shown in Figure 2. The spectral region of interest, from 950 – 1020 cm^{-1}, is the range within which the uranyl ν_3 frequencies appear for these $UO_2(L)_3^{2+}$ complexes. The ν_3 bands are characteristically sharp, with peak widths (fwhm) of <20 cm^{-1} using the experimental conditions employed here. The only other absorptions apparent in Figure 2 are the narrow (~14 cm^{-1} fwhm) peak at 750 cm^{-1} for $UO_2(tmu)_3^{2+}$ and the broader (~30 cm^{-1} fwhm) peak at 920 cm^{-1} for $UO_2(dmso)_3^{2+}$. Both of these latter features are assigned to ligand vibrational modes.

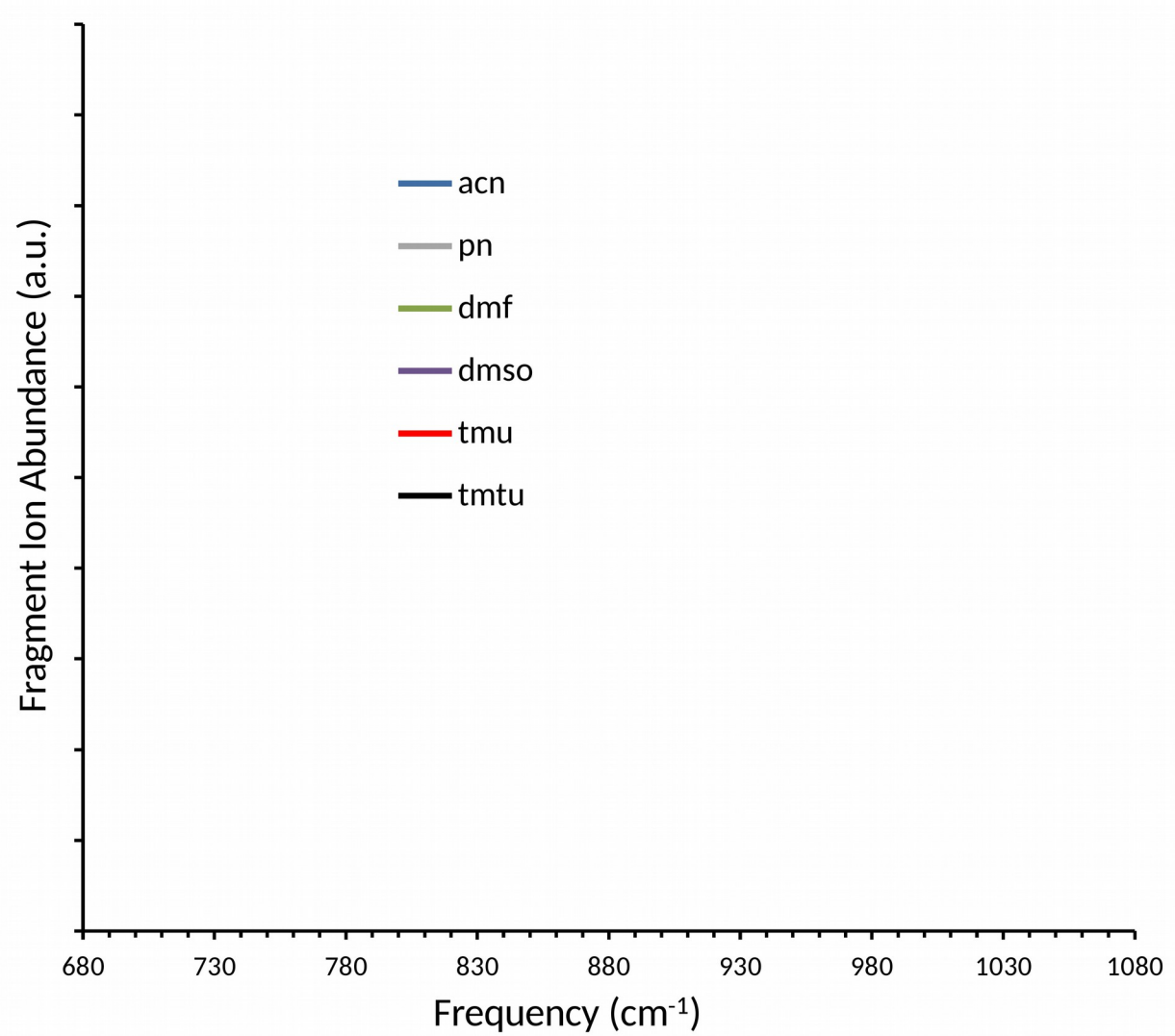

Figure 2. Experimental IRMPD spectra for $UO_2(L)_3^+$ complexes. The sharp and intense ν_3 absorption bands are in the range of 950 – 1020 cm^{-1}. The only other intense features are due to ligand modes for $UO_2(tmu)_3^+$ around 740 cm^{-1} and $UO_2(dmso)_3^+$ around 920 cm^{-1}. An expansion of the 880 – 1060 cm^{-1} region of these spectra is shown in Figure 3a.

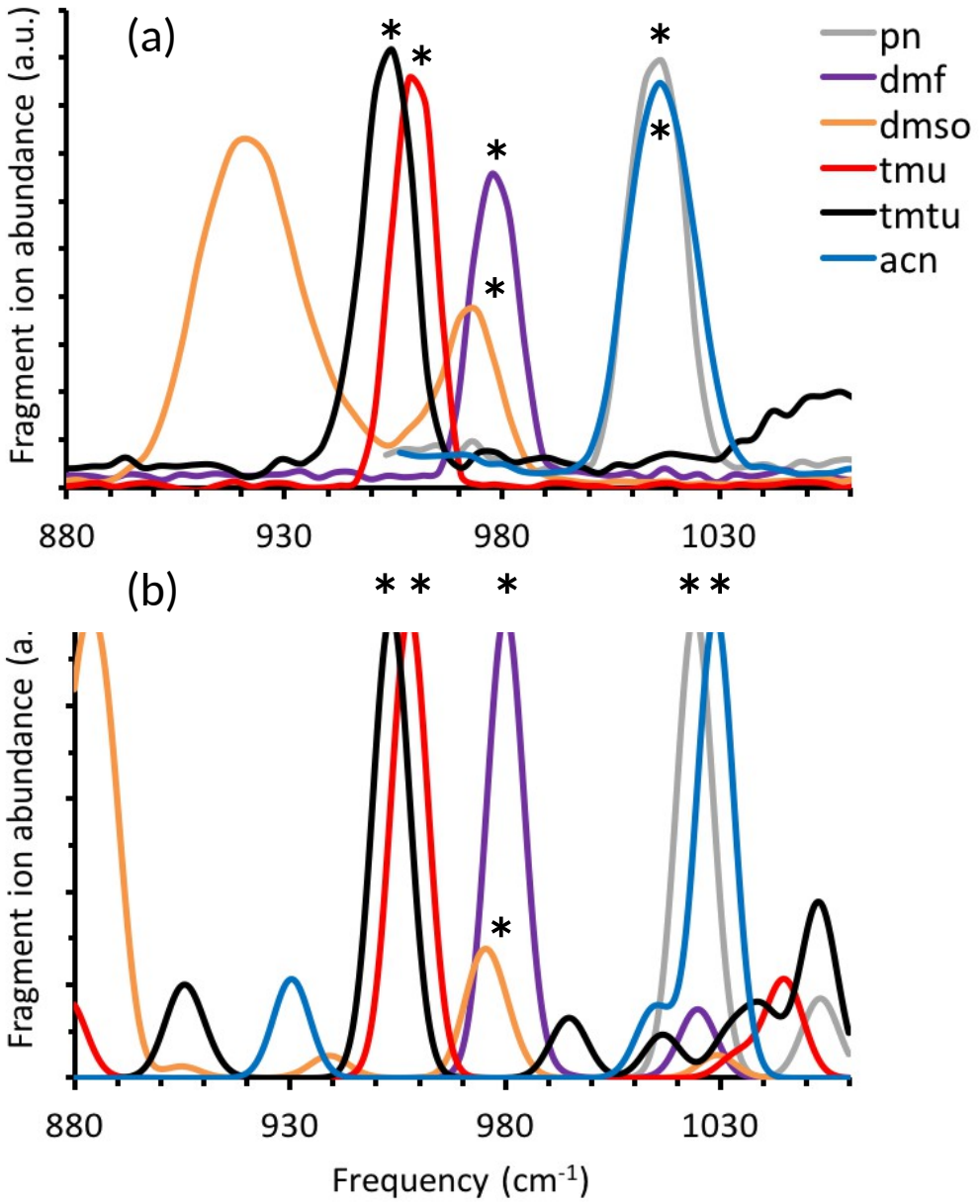

Figure 3. Experimental (a) and B3LYP computed (b) IR spectra for $UO_2(L)_3^{2+}$ complexes. The computed IR spectra are normalized to the max peak value. The ν_3 absorption bands are identified by asterisks.

The IRMPD spectra for the $UO_2(L)_3^{2+}$ complexes in the narrow ν_3 spectral range of interest are shown in Figure 3a. The broad peak at 920 cm^{-1} attributed to a ligand vibrational mode remains apparent in the $UO_2(dmso)_3^{2+}$ spectrum. The corresponding computed spectra, obtained with from the scaled B3LYP frequencies, are shown in Figure 3b. Comparison of

Figures 3a and 3b reveals that although the computed spectra do not rigorously predict the experimental results, the experiment/theory agreement for the asymmetric uranyl □3 is rather good. In particular, the computed spectra accurately reproduce the following ordering of □3 for the computed $UO_2(L)_3^{2+}$: L = acn > pn > aco > dmf > dmso > tmu. The tmtu □3 is found to be 2 cm^{-1} below the tmu □3 in the experiment. In the computed results this same order is found for the tmtu complex with one ligand bidentate bonded, whereas the monodentate bonded tmtu complex has a □3 that is computed to be slightly larger than tmu. For tmtu an additional spectrum was measured over the broader energy range from 880 cm^{-1} to 1750 cm^{-1}, and compared to the calculated spectra of the two bonding motifs for the tmtu complex in an attempt to identify the complex that was actually observed. The experimental and computed spectra are shown in Figure 4.

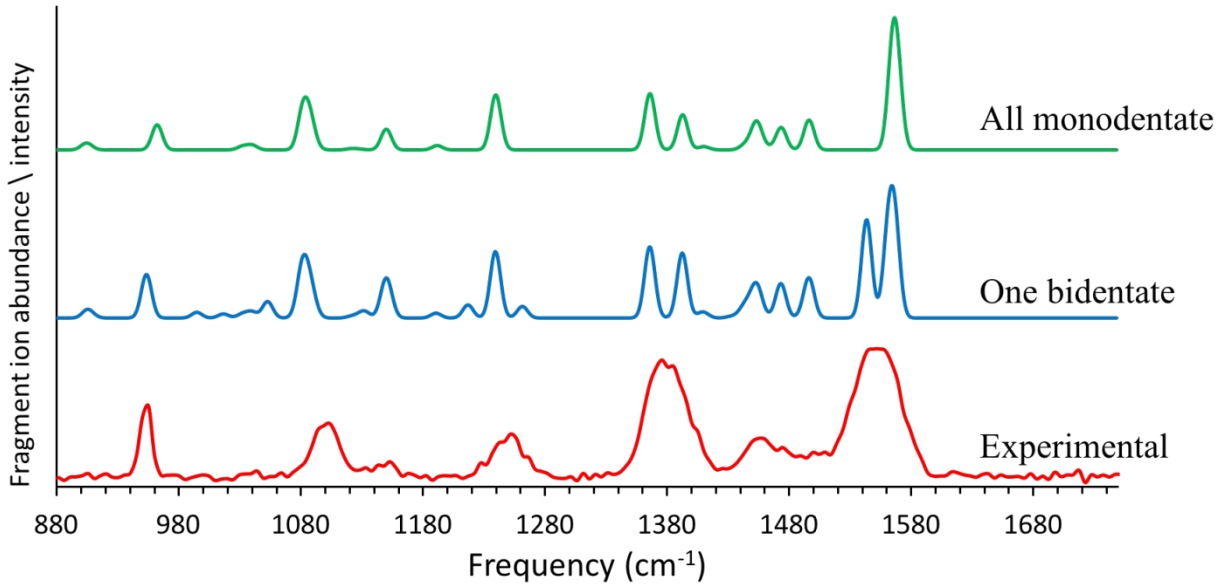

Figure 4. Experimental IR spectra for $UO_2(tmtu)_3^{2+}$ complex, combined with the B3LYP computed spectra for the two binding motifs shown in Figure 1. The computed IR spectra are normalized to the maximum peak intenisty.

The two computed spectra for tmtu with different bonding motifs in Figure 4 are similar, with the exception of the additional peak for the complex with one bidentate bonded ligand in the 1520-1600 cm^{-1} range that could account for the experimentally observed broadening at the same frequency. The additional spectral feature plus the better alignment of the □3 with the experimental tmtu spectrum, as well as its proper ordering compared to other calculated and

experimental data, suggest that the experimentally observed complex has one ligand bidentate bonded, in accord with this being the computed lowest-energy structure.

The measured and computed ν_3 are given in Table 1, where the experimental value for $UO_2(aco)_3^{2+}$ is from ref.[7] The maximum difference between the experimental and B3LYP computed (and scaled) ν_3 is 12 cm^{-1} for L = acn, and the average difference for the seven computed complexes is 4 cm^{-1}. It is apparent that the computations quite effectively predict the actual ν_3 for these complexes, providing confidence in validity of the computed structures shown in Figure 1.

4.3 Correlation between Uranyl Asymmetric Stretch Frequencies and Ligand Proton Affinities

As discussed above, it has previously been demonstrated that the red-shift in ν_3 qualitatively indicates the degree of electron donation from equatorial coordinating ligands to the uranium metal center in uranyl.[1-4,7] Whereas the library of MCAs is sparse, PAs have been determined for many molecules. PAs are generally much higher than MCAs, largely due to the covalent nature of proton-ligand bonding versus the primarily electrostatic—i.e. electron donor—nature of metal ion-ligand bonding. The measured ν_3 for $UO_2(L)_3^{2+}$ comprising ligands having a range of PAs provides an evaluation of the PA parameter as an indicator of ligand-to-uranyl electron donation.

A plot of the measured ν_3 for $UO_2(L)_3^{2+}$ versus PA[L] is shown in Figure 5. The uncertainties are assigned as ±2 cm^{-1} for the experimental ν_3 and ±8 kJ/mol for the PAs; this latter uncertainty is recommended for absolute PAs[28] and the uncertainty in most of the relative values is likely smaller but indeterminate.[30] It is apparent that there is a rather good correlation between ν_3 and PA over this relatively broad range of values. The indicated linear relationship is remarkably good—the underlying basis for the linear correlation between these two variables is not obvious. It is expected that the U=O bond strength, indicated by the O=U=O stretch frequency ν_3, is diminished by charge donation to the uranium metal center, which is associated with the ligand PA. However, neither of these relationships—bond strength versus ν_3 nor bond strength versus PA—is necessarily expected to be first order, such that the seemingly fortuitous overall linear relationship in Figure 5 is notable.

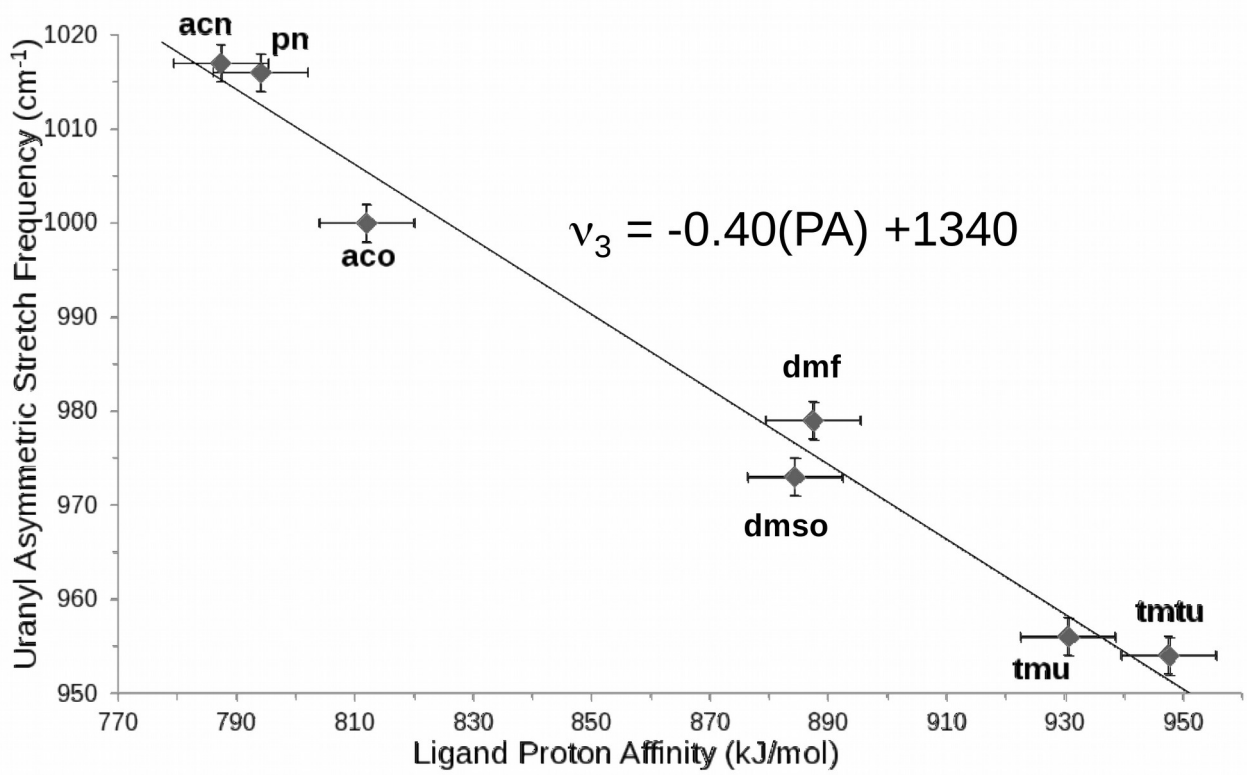

Figure 5. Linear correlation between measured $\nu_3[UO_2(L)_3^{2+}]$ and PA[L].

Despite the overall good linear relationship between ν_3 and PA evident in Figure 5 there are significant deviations from the correlation, particularly for ligands having similar PAs. Although for consistency the assigned uncertainties of ±8 kJ/mol result in overlap of the ranges of PA[pn] and PA[acn], Williams et al. have demonstrated that the former is 10 kJ/mol higher than the latter.[29] However, the ν_3 for the acn and pn complexes are essentially the same to within the experimental accuracy. The PA[dmso] and PA[dmf] are very close in energy. However, for the observed trend to hold the ν_3 of dmf should have been below that of dmso, but experimentally the order is reversed. It is interesting to look at the calculated PAs in Table 1. Each of them are within 3 kJ/mol from the experimental values, with the exception of dmso. The PA[dmso] is calculated to be 15 kJ/mol higher then experiment. This could be an artifact of the computational model used,[31] though the agreement of the calculated PA to experiment for the remaining complexes, including other sulfur containing ligands, is remarkable. Finally, PA[tmtu] is higher than PA[tmu] but ν_3 for $UO_2(tmtu)_3^{2+}$ is only 2 cm^{-1} below that of $UO_2(tmu)_3^{2+}$, a difference within the experimental uncertainty. The computed structure of $UO_2(tmtu)_3^{2+}$ reveals

that one of the three ligands is bidentate such that even greater electron donation, and a greater ν_3 red-shift than predicted from PA[tmtu]—which corresponds to monodentate coordination of a proton to the carbonyl sulfur[32]—would be expected, the opposite of the observed deviation from the linear fit in Figure 5. These examples reveal that caution must be exercised in applying an apparently good correlation that appears as valid over a broad range of parameters to particular complexes that have relatively similar values of these parameters. Although there is a correlation between ν_3 and PA, it is apparent that the overall ν_3 versus PA correlation in Figure 5 cannot be employed to predict the comparative red-shift in ν_3 for ligands having similar PAs. Conversely, PAs cannot be reliably inferred from comparative red-shifts in ν_3. This failure implies that PA is not necessarily a quantitatively reliable indicator of electron donation to metal ions, although there apparently is a relationship between these properties. The deviations from the correlation at a fine level are not surprising in view of the very different nature of binding of protons and metal ions to electron-donor ligands, as remarked above. It is perhaps more surprising that the correlation is as good as found.

The computed U=O_{yl} bond distances (Table 2) also exhibit a correlation with PA, and thus ν_3, as might be expected because bond distances *generally* increase as bond strengths decrease.[33] The average calculated U=O_{yl} bond distance in $UO_2(L)_3^{2+}$ increases from 1.74 Å for L = pn, to 1.76 Å for L = dmso and dmf, to 1.77 Å for L = tmu and tmtu. For comparison, the bond distances computed here for bare uranium dioxides are 1.70 Å for UO_2^{2+}, 1.76 Å for UO_2^{+} and 1.78 Å for UO_2; increasing electron density results in reduced bond strength and concomitant bond elongation. It is known that the bond dissociation energy decreases in $[O=U=O]^{n+}$ molecules as *n* decreases from 2+ to zero.[34] Based on the U=O_{yl} bond distances, it can be inferred that the effective charge on uranyl in $UO_2(tmu)_3^{2+}$ and $UO_2(tmtu)_3^{2+}$ is intermediate between that of UO_2^{+} and neutral UO_2. This result indicates substantial charge donation from the ligands and is in accord with the underlying thesis of decreasing bond strength with increasing charge donation in uranyl coordination complexes.

4.4 Assessing the Correlation for Uranyl Coordinated by Polydentate Ligands

The PA of the polycyclic ether 15-crown-5 (15C5) has been determined as 933 kJ/mol,[35] which is similar to that of tmu (931 kJ/mol). Based on the correlation in Figure 1 it is thus predicted that ν_3 for hypothetical $UO_2(15C5)_3^{2+}$ should be close to the value of 956 cm^{-1}

determined for $UO_2(tmu)_3^{2+}$. The previously measured ν_3 for $UO_2(15C5)_2^{2+}$, the uranyl complex with two 15C5 ligands, is 976 cm^{-1},[13] which is ~20 cm^{-1} higher than predicted from the PA correlation for the complex with an additional 15C5 ligand. A red-shift of 17 cm^{-1} has been reported for addition of an aco ligand to $UO_2(aco)_2^{2+}$ such that a red-shift on the order of 20 cm^{-1}, to ca. 956 cm^{-1}, appears reasonable for hypothetical addition of a 15C5 ligand to $UO_2(15C5)_2^{2+}$. It should be noted that in $UO_2(15C5)_2^{2+}$ the uranium is coordinated by six oxygen atoms, three from each 15C5 ligand in a sandwich-like structure,[13] such that effective coordination by a third 15C5 ligand would likely not be feasible.

A notable result is that ν_3 for $UO_2(15C5)_2^{2+}$, in which there are six U-O_{eq} bonds, is essentially the same as ν_3 for $UO_2(dmf)_3^{2+}$ and $UO_2(dmso)_3^{2+}$, in which there are three U-O_{eq} bonds. In the $UO_2(15C5)_2^{2+}$ sandwich structure complex it is challenging to achieve effective coordination by all donor sites of the large crown ligands; the three relative short U-O_{eq} bond distances in $UO_2(15C5)_2^{2+}$ are 2.57, 2.66 and 2.70 Å for each 15C5, resulting in hexadentate coordination of uranium. For comparison with the B3LYP computed structures here, the average U-O_{eq} distances in $UO_2(dmso)_3^{2+}$, $UO_2(dmf)_3^{2+}$ and $UO_2(tmu)_3^{2+}$are 2.28, 2.30 and 2.26 Å, respectively, indicating a substantially stronger (electrostatic) bonding interaction with the ketone oxygen in these ligands than with any of the ether oxygens in 15C5. Each of the three dmso, dmf and tmu ketone oxygens can effectively bind to uranyl in the equatorial plane. Only six of the ten 15C5 oxo groups bind to uranyl, and relatively inefficiently as indicated by the substantially longer U-O_{eq} bond distances. Given the very different ligand coordination in $H15C5^+$ (monodentate[35]) and $UO_2(15C5)_2^{2+}$ (tridentate[13]) it is remarkable that the correlation between PA and ν_3 evidently remains essentially valid. This result can be attributed to the reduced efficacy of tridentate coordination in the 15C5 complex. It is not expected that the correlation between PA and ν_3 should remain generally valid for polydentate ligands.

The previously reported most extreme red shift for a dipositive uranyl complex was to ν_3 = 965 cm^{-1} for $UO_2(TMOGA)_2^{2+}$ where TMOGA = tetramethyl-3-oxa-glutaramide, a strongly binding tridentate oxygen-donor ligand,[12] which is 23 cm^{-1} below the previous record shift for $UO_2(aco)_2^{2+}$.[7] The present results reveal a further red-shift below 965 cm^{-1} of ~10 cm^{-1} due to three monodentate ligands in both $UO_2(tmu)_3^{2+}$ and $UO_2(tmtu)_3^{2+}$. An even larger red-shift is predicted for $UO_2(tmtu)_4^{2+}$, with a calculated ν_3 equal to 932 cm^{-1}. The extent of charge donation in these two complexes to the *formally* dipositive uranyl metal center is evidently unprecedented.

These results indicate greater charge donation from three monodentate oxygen-donor tmu ligands than from two tridentate TMOGA ligands. The distances between uranium and the coordinating ligand sites in $UO_2(TMOGA)_2^{2+}$ are 2.38 Å for U-O_{ketone} and 2.77 Å for U-O_{ether}. The former distance is ~0.1 Å longer than the U-O_{ketone} distances in the complexes with three dmso, dmf and tmu ligands; the U-O_{ether} distance in the TMOGA complex is substantially longer. Comparison of the ν_3 frequencies and the U-O_{eq} distances for the $UO_2(L)_3^{2+}$ complexes with those for $UO_2(15C5)_2^{2+}$ and $UO_2(TMOGA)_2^{2+}$ clearly reveals that each of the oxygen donor atoms in the monodentate ligands (and for the tmtu one bidentate ligand) bind considerably more effectively to uranyl than do the oxygens in the tridentate ligands.

5. Conclusions

The proton affinity (PA) of an organic molecule is its binding energy (enthalpy) to a proton in the gas phase. The binding of a proton to a donor site in a molecule is qualitatively very different than the binding of a metal cation to the same molecule, which may have multiple donor sites. It was here demonstrated that there is a good correlation between ligand PA and ν_3 for several $UO_2(L)_3^{2+}$ complexes. Rather remarkably, this correlation between PA[L] and ν_3 is linear. Because the red-shift of ν_3 indicates charge donation to uranyl, this relationship suggests that PA can predict uranyl cation affinity (UCA) towards a ligand. Although the correlation is valid over a broad range of PA values, significant deviations were found for ligands with similar PAs, possibly due to partially non-electrostatic (i.e. covalent) bonding.

The ligands studied here were predominantly monodentate, with only one viable metal (or proton) binding site. Comparison with previously studied polydentate ligands reveals a much less effective interaction per donor site due to steric constraints that preclude optimal coordination and bonding interactions for the multiple sites.

It has been confirmed and elaborated that the red-shift of ν_3 in gas-phase uranyl complexes is an indicator of the degree of ligand charge donation. Furthermore, ligand PAs can qualitatively predict the extent of this donation for the ligands with single donor sites studied here. It is shown that this predictive capability breaks down when ligands with multiple donor sites are considered.

Supporting Information

Raw calculated structures, frequencies, energies and derived coordination energies, proton affinities and asymmetric stretch frequencies for all complexes considered.

Acknowledgements

Research supported as part of the Center for Actinide Science and Technology (CAST) an Energy Frontier Research Center (EFRC) funded by the U.S. Department of Energy (DOE), Office of Science, Basic Energy Sciences (BES), under Award Number DE-SC0016568 (J.K.G.: devised and led the experiments, and wrote the manuscript with W.A.dJ.), by start-up funds from the Bayer School of Natural and Environmental Sciences and Duquesne University (M.V.S), and by the Netherlands Organisation for Scientific Research under vici-grant no. 724.011.002 and the Stichting Physica (J.O.). This research used resources of the National Energy Research Scientific Computing Center (NERSC), which is supported by the Office of Science of the U.S. Department of Energy under Contract No. DE-AC02-05CH11231. Some of the calculations were performed using the Oak Ridge Leadership Computing Facility, which is a DOE Office of Science User Facility supported under Contract DE-AC05-00OR22725. An award of computer time was provided by the Innovative and Novel Computational Impact on Theory and Experiment (INCITE) program. We gratefully acknowledge the *Nederlandse Organisatie voor Wetenschappelijk Onderzoek* (NWO) for the support of the FELIX Laboratory.

References

(1) Mcglynn, S. P.; Neely, W. C.; Smith, J. K.: Electronic Structure, Spectra, and Magnetic Properties of Oxycations. 3. Ligation Effects on Infrared Spectrum of Uranyl Ion. *J. Chem. Phys.* **1961**, *35*, 105-116.

(2) Basile, L. J.; Sullivan, J. C.; Ferraro, J. R.; Labonville, P.: Raman-Scattering of Uranyl and Transuranium V, Vi, and Vii Ions. *Appl. Spectrosc.* **1974**, *28*, 142-145.

(3) Nguyentrung, C.; Begun, G. M.; Palmer, D. A.: Aqueous Uranium Complexes. 2. Raman-Spectroscopic Study of the Complex-Formation of the Dioxouranium(Vi) Ion with a Variety of Inorganic and Organic-Ligands. *Inorg. Chem.* **1992**, *31*, 5280-5287.

(4) Sarsfield, M. J.; Helliwell, M.; Raftery, J.: Distorted equatorial coordination environments and weakening of U=O bonds in uranyl complexes containing NCN and NPN ligands. *Inorg. Chem.* **2004**, *43*, 3170-3179.

(5) Di Pietro, P.; Kerridge, A.: U-O-yl Stretching Vibrations as a Quantitative Measure of the Equatorial Bond Covalency in Uranyl Complexes: A Quantum-Chemical Investigation. *Inorg. Chem.* **2016**, *55*, 573-583.

(6) Schnaars, D. D.; Wilson, R. E.: Lattice Solvent and Crystal Phase Effects on the Vibrational Spectra of UO2Cl42-. *Inorg. Chem.* **2014**, *53*, 11036-11045.

(7) Groenewold, G. S.; Gianotto, A. K.; Cossel, K. C.; Van Stipdonk, M. J.; Moore, D. T.; Polfer, N.; Oomens, J.; de Jong, W. A.; Visscher, L.: Vibrational spectroscopy of mass-selected [UO2(ligand)(n)] (2+) complexes in the gas phase: Comparison with theory. *J. Am. Chem. Soc.* **2006**, *128*, 4802-4813.

(8) Bouchoux, G.; Salpin, J. Y.: Gas-phase basicities of polyfunctional molecules. Part 2: Saturated basic sites. *Mass Spec. Rev.* **2012**, *31*, 353-390.

(9) Woodin, R. L.; Houle, F. A.; Goddard, W. A.: Nature of Bonding of Li+ to H2O and NH3 - Ab-Initio Studies. *Chem. Phys.* **1976**, *14*, 461-468.

(10) Burk, P.; Koppel, I. A.; Koppel, I.; Kurg, R.; Gal, J. F.; Maria, P. C.; Herreros, M.; Notario, R.; Abboud, J. L. M.; Anvia, F.; Taft, R. W.: Revised and expanded scale of gas-phase lithium cation basicities. An experimental and theoretical study. *J. Phys. Chem. A* **2000**, *104*, 2824-2833.

(11) McMahon, T. B.; Ohanessian, G.: An experimental and ab initio study of the nature of the binding in gas-phase complexes of sodium ions. *Chem. Eur. J.* **2000**, *6*, 2931-2941.

(12) Gibson, J. K.; Hu, H. S.; Van Stipdonk, M. J.; Berden, G.; Oomens, J.; Li, J.: Infrared Multiphoton Dissociation Spectroscopy of a Gas-Phase Complex of Uranyl and 3-Oxa-Glutaramide: An Extreme Red-Shift of the [O=U=O](2+) Asymmetric Stretch. *J. Phys. Chem. A* **2015**, *119*, 3366-3374.

(13) Hu, S. X.; Gibson, J. K.; Li, W. L.; Van Stipdonk, M. J.; Martens, J.; Berden, G.; Redlich, B.; Oomens, J.; Li, J.: Electronic structure and characterization of a uranyl di-15-crown-5 complex with an unprecedented sandwich structure. *Chem. Comm.* **2016**, *52*, 12761-12764.

(14) Valle, J. J.; Eyler, J. R.; Oomens, J.; Moore, D. T.; van der Meer, A. F. G.; von Helden, G.; Meijer, G.; Hendrickson, C. L.; Marshall, A. G.; Blakney, G. T.: Free electron laser-Fourier transform ion cyclotron resonance mass spectrometry facility for obtaining infrared multiphoton dissociation spectra of gaseous ions. *Rev. Sci. Instrum.* **2005**, *76*, 0231031-0231037.

(15) Bagratashvili, V. N.; Letokov, V. A.; Makarov, A. A.; Ryabov, E. A.: *Multiple Photon Infrared Laser Photophysics and Photochemistry*; Harwood Chur: Switzerland, 1985.

(16) Oomens, J.; Tielens, A. G. G. M.; Sartakov, B. G.; von Helden, G.; Meijer, G.: Laboratory infrared spectroscopy of cationic polycyclic aromatic hydrocarbon molecules. *Astrophys. J.* **2003**, *591*, 968-985.

(17) Kamrath, M. Z.; Garand, E.; Jordan, P. A.; Leavitt, C. M.; Wolk, A. B.; Van Stipdonk, M. J.; Miller, S. J.; Johnson, M. A.: Vibrational Characterization of Simple Peptides Using Cryogenic Infrared Photodissociation of H-2-Tagged, Mass-Selected Ions. *J. Am. Chem. Soc.* **2011**, *133*, 6440-6448.

(18) Gao, J. H.; Berden, G.; Rodgers, M. T.; Oomens, J.: Interaction of Cu+ with cytosine and formation of i-motif-like C-M+-C complexes: alkali versus coinage metals. *Phys. Chem. Chem. Phys.* **2016**, *18*, 7269-7277.

(19) Valiev, M.; Bylaska, E. J.; Govind, N.; Kowalski, K.; Straatsma, T. P.; Van Dam, H. J. J.; Wang, D.; Nieplocha, J.; Apra, E.; Windus, T. L.; de Jong, W.: NWChem: A comprehensive and scalable open-source solution for large scale molecular simulations. *Comput. Phys. Commun.* **2010**, *181*, 1477-1489.

(20) Slater, J. C.: A Simplification of the Hartree-Fock Method. *Phys. Rev.* **1951**, *81*, 385-390.

(21) Vosko, S. H.; Wilk, L.; Nusair, M.: Accurate spin-dependent electron liquid correlation energies for local spin density calculations: a critical analysis. *Can. J. Phys.* **1980**, *58*, 1200-1211.

(22) Becke, A. D.: *J. Chem. Phys.* **1992**, *98*, 1372.

(23) Lee, C.; Yang, W.; Parr, R. G.: Development of the Colle-Salvetti correlation-energy formula into a functional of the electron density. *Phys. Rev. B* **1988**, *37*, 785-789.

(24) Kuchle, W.; Dolg, M.; Stoll, H.; Preuss, H.: Energy-Adjusted Pseudopotnetials for the Actinides - Parameter Sets and Test Calculations for Thorium and Thorium Monoxide. *J. Chem. Phys.* **1994**, *100*, 7535-7542.

(25) Godbout, N.; Salahub, D. R.; Andzelm, J.; Wimmer, E.: Optimization of Gaussian-Type Basis Sets for Local Spin-Denisty Calculations. 1. Boron through Neon, Optimization Technique and Validation. *Can. J. Chem.* **1992**, *70*, 560-571.

(26) McQuarrie, D. A.; Simon, J. D.: *Molecular Thermodynamics*; University Science Books: Sausalito, California, 1999.

(27) ElAzhary, A. A.; Suter, H. U.: Comparison between optimized geometries and vibrational frequencies calculated by the DFT methods. *J. Phys. Chem.* **1996**, *100*, 15056-15063.

(28) Hunter, E. P. L.; Lias, S. G.: Evaluated gas phase basicities and proton affinities of molecules: An update. *J. Phys. Chem. Ref. Data* **1998**, *27*, 413-656.

(29) Williams, T. I.; Denault, J. W.; Cooks, R. G.: Proton affinity of deuterated acetonitrile estimated by the kinetic method with full entropy analysis. *Int. J. Mass Spec.* **2001**, *210*, 133-146.

(30) Nourse, B. D.; Cooks, R. G.: Proton Affinity Determinations Using the Kinetic Method in an Ion Trap Mass-Spectrometer. *International Journal of Mass Spectrometry and Ion Processes* **1991**, *106*, 249-272.

(31) Turecek, F.: Proton affinity of dimethyl sulfoxide and relative stabilities of C2H6OS molecules and C2H7OS+ ions. A comparative G2(MP2) ab initio and density functional theory study. *J. Phys. Chem. A* **1998**, *102*, 4703-4713.

(32) Abboud, J. L. M.; Mo, O.; Depaz, J. L. G.; Yanez, M.; Esseffar, M.; Bouab, W.; Elmouhtadi, M.; Mokhlisse, R.; Ballesteros, E.; Herreros, M.; Homan, H.; Lopezmardomingo, C.; Notario, R.: Thiocarbonyl Versus Carbonyl-Compounds - a Comparison of Intrinsic Reactivities. *J. Am. Chem. Soc.* **1993**, *115*, 12468-12476.

(33) Kaupp, M.; Danovich, D.; Shaik, S.: Chemistry is about energy and its changes: A critique of bond-length/bond-strength correlations. *Coordination Chemistry Reviews* **2017**, *344*, 355-362.

(34) Marçalo, J.; Gibson, J. K.: Gas-Phase Energetics of Actinide Oxides: An Assessment of Neutral and Cationic Monoxides and Dioxides from Thorium to Curium. *J. Phys. Chem. A* **2009**, *113*, 12599-12606.

(35) Sharma, R. B.; Blades, A. T.; Kebarle, P.: Protonation of Polyethers, Glymes and Crown Ethers, in the Gas-Phase. *J. Am. Chem. Soc.* **1984**, *106*, 510-516.

Graphical Abstract

Measured and computed infrared spectra of gas-phase uranyl coordination complexes reveal a remarkably good linear correlation between ligand proton affinity and uranyl asymmetric stretch frequency.